LATTICE-BOLTZMANN SIMULATION OF TWO-PHASE FLUID FLOW THROUGH POROUS MEDIA

Carlos E. Pico
capico@lmpt.ufsc.br

Luis O. E. dos Santos
emerich@lmpt.ufsc.br

Paulo C. Philippi
philippi@lmpt.ufsc.br

Universidade Federal de Santa Catarina
Laboratório de Meios Porosos e Propriedades Termofísicas
Campus Universitário - Trindade
Florianópolis/SC - Brasil - 88040-900

Abstract. *The two-phase fluid flow in porous media was analyzed by simulations using the Lattice-Boltzmann Method, with a model for ideal immiscible fluids, based in a split collision operator. The method was applied to flows through simple two dimensional geometries to investigate the capillary number and wettability functionality of the conventional relative permeability. We use randomly generated initial conditions to avoid the effect of flow history and a uniform body force to drive the two fluids trough the porous media. The results of this steady state numerical experiments agree qualitatively with similar experiments reported in literature and show that the Lattice-Boltzmann model implemented can simulate realistic two-phase fluid flow in complex geometries.*

Keywords: *Lattice-Boltzmann method, Transport in porous media, Two phase flow, Relative permeability.*

1. Introduction

The fluid flow through porous media is a field of considerable scientific and technological interest (e.g. oil recovery). At the moment, the theory for single phase flow in porous media is in a stage of relative maturity. On the other hand, a consistent theoretical description of two phase flow does not exist, due to the difficulty in analyzing complex interface dynamics and fluid solid interactions. Usually, two-phase flow in porous media is described by Darcy's law for isotropic media, written for phase i as

$$\mathbf{u}_i = \frac{k k_{ri}\left(S_i\right)}{\mu_i}\left(-\nabla P_i + \rho_i \mathbf{g}\right), \tag{1}$$

where $\mathbf{u}_i$ is the volumetric average velocity, μ_i is the viscosity, k is the intrinsic permeability, k_{ri} is the conventional relative permeability (dependent solely on the phase i saturation, S_i) and ∇P_i and $\rho_i \mathbf{g}$ are the pressure gradient and the body force, respectively. The former expression is an extension of the Darcy's law for single phase fluid flow in porous media, based on the assumption that each phase flows in separate channels, limited by stable interfaces. Experimentally, it has been demonstrated that the assumption behind the generalization of Darcy's law for immiscible fluids is not valid in a wide range of flow parameters and, in consequence, the relative permeability dependence only on the saturation and even the linearity of Eq. (1) are highly questionable.

In spite of the problems mentioned above, the relative permeability is a useful concept in oil industry, where it is determined experimentally for use in economical analysis and simulations of reservoirs. For practical use of the generalized Darcy's law, the effect of other parameters, as viscosity ratio M, equilibrium contact angle θ^{eq}, capillary number Ca and flow history in relative permeability should be included [Avraam and Payatakes, 1995, Dullien, 1992].

Pore scale simulations using Lattice Boltzmann techniques could improve our understanding of transport phenomena in porous media. Due to its kinetic nature, the evolution of a particle distribution function can be described in terms of local collisions with solid sites using simple bounce-back boundary conditions, easily implemented for flow in complex geometries [van Genabeek and Rothman, 1996, Olson and Rothman, 1997].

In this paper, simulation is performed using a Lattice Boltzmann model for ideal immiscible fluids, for steady state two phase flow (similar to the steady state experiment for the determination of relative permeability) in a simplified porous media, to study the effect of the capillary number and the equilibrium contact angle in relative permeabilities.

2. The Lattice Boltzmann Method for immiscible fluids

The Lattice Boltzmann Method (LBM) is a relatively new tool for the simulation of incompressible fluid flow, based on a special discretization of the continuous Boltzmann equation [He and Luo, 1997]. In this numerical method, a particle distribution function f_i, defined in specific sites $\mathbf{X}$ of a regular lattice, connected by a set of velocity vectors $\{\mathbf{c}_i\}$, evolve following a Lattice Boltzmann Equation (LBE) with a model for the collision operator Ω_i. The most frequently used model is the Bhatnagar-Gross-Krook that results in the single relaxation time or LBGK equation [Qian et al., 1992].

Because of its mesoscopic character, the LBM is suitable for the macroscopic description of microscopic interactions, as interface dynamics and capillary phenomena [dos Santos et al., 2005]. There are different LBM approaches to the hydrodynamics of athermal two-phase fluid flow, some of them recently reviewed by [He and Doolen, 2002]. In this paper a split collision operator is used as a collision model for two ideal fluids [Facin, 2003, Santos et al., 2003]. The collision operator was splitted to treat explicitly collisions among particles of the same and different species, as in kinetic theory of mixtures, and each term is considered as a BGK like model. The Lattice Boltzmann equation for specie k ($k = r, b$) is

$$K_i\left(\mathbf{X}+\mathbf{c}_i, t+1\right) - K_i\left(\mathbf{X}, t\right) = \Omega_i^k \tag{2}$$

with

$$\Omega_i^r = \Omega_i^{rr} + \Omega_i^{rb} = \omega^r \frac{R_i^{eq}\left(\rho^r, \mathbf{u}^r\right) - R_i}{\tau^r} + \omega^b \frac{R_i^{eq}\left(\rho^r, \vartheta^b\right) - R_i}{\tau^m}, \tag{3}$$

$$\Omega_i^b = \Omega_i^{br} + \Omega_i^{bb} = \omega^r \frac{B_i^{eq}\left(\rho^b, \vartheta^r\right) - B_i}{\tau^m} + \omega^b \frac{B_i^{eq}\left(\rho^b, \mathbf{u}^b\right) - B_i}{\tau^b}, \tag{4}$$

where ω^k is the local concentration of species k and the macroscopic properties ρ^k and $\mathbf{u}^k$ are calculated as velocity moments of the respective distribution function [He and Luo, 1997]. The cross collision term ($\Omega_i^{kk'}$) relax the distribution of k particles to a velocity $\vartheta^{k'}$, equal to the velocity of k' particles modified by an antidiffusive term, that mimics the effect of an attractive force field

$$\vartheta^{k'} = \mathbf{u}^{k'} + A\hat{\mathbf{g}^{k'}}, \tag{5}$$

where A is an interaction factor that controls the strength of interfacial tension and $\hat{\mathbf{g}^{k'}}$ is a unitary vector opposed to the local gradient of $\omega^{k'}$. The vector $\hat{\mathbf{g}^{k'}}$ is calculated as

$$\hat{\mathbf{g}^b} = -\hat{\mathbf{g}^r} = \begin{cases} \dfrac{\sum_i \omega^r(\mathbf{X}+\mathbf{c}_i,t)\mathbf{c}_i}{\left|\sum_i \omega^r(\mathbf{X}+\mathbf{c}_i,t)\mathbf{c}_i\right|} & \text{when } \left|\sum_i \omega^r\left(\mathbf{X}+\mathbf{c}_i,t\right)\mathbf{c}_i\right| \neq 0 \\ 0 & \text{otherwise} \end{cases}. \tag{6}$$

In a similar way, the interaction between each fluid and the solid boundary is modeled by assuming that the wall sites have a value ω^{sr}, representing the affinity between solid and r particles. The no-slip boundary condition at solid-fluid interfaces is realised by the half-way bounce-back boundary condition, where the momenta of the fluid particles meeting a solid wall are simply reversed during the propagation step. The bounce-back rule is simple and computationally efficient, and enables fluid flow simulations in complex geometries.

A more detailed description and validation of the method, and a first order Chapman-Enskog analysis with expressions for viscosity, interfacial tension and interface width could be found in references [Facin, 2003, Santos et al., 2003, dos Santos et al., 2005].

3. Simulation setup

The simulation was carried out in a bi-dimensional porous medium, qualitatively similar to chamber-and-throat type networks [Avraam and Payatakes, 1995]. The medium had 400x400 lattice sites with ~42% porosity and was composed of 32 identical chambers, in a square lattice, connected by channels with periodic boundary conditions in all directions (see Fig. 1).

To avoid the effect of the saturation history, each site was initialized, with r or b distribution, randomly with probability equal to the desired saturation. The small drops coalesce while the two fluids are forced along the x direction with the same body force until the saturation of k, defined as

$$S_k = \frac{\text{number of sites with } \omega^k > 0.5}{\text{number of fluid sites}}, \tag{7}$$

Table 1. Simulation parameters. In all cases the relaxation parameters, the viscosities and initial densities are equal ($\tau^r = \tau^b = \tau^m = 1.0$, $\nu^r = \nu^b = 1/6$ and $\rho_0^r = \rho_0^b = 1.0$)

Ca^I	$4E-4$	σ^I	$1/6$	θ^I	0
Ca^{II}	$4E-3$	σ^{II}	$1/6$	θ^{II}	~50
Ca^{III}	$5E-3$	σ^{III}	$1/4$	θ^{III}	~75

and the total mass flux of species k,

$$Q_k = \sum_{\text{all sites}} \rho^k \mathbf{u}^k \tag{8}$$

reaches the stationary state.

In general, the stationary state was attained after 250000 steps. After this, the simulation continued for more 50000 time steps, that were used to get the average value and the standard deviation of the saturation and total flux. As in real experiments, the macroscopic variables are highly noisy (with constant time averaged values), particularly at low and medium saturations of the non wetting fluid. In these cases, the coalescence and break up of ganglia and drops are more frequent [Avraam and Payatakes, 1995]. The previous procedure was repeated for various saturations considering three different capillary numbers, with three different wettabilities. For simplicity and computational efficiency the initial densities and the relaxation parameters τ^r, τ^b and τ^m (and correspondingly, the viscosities of the two fluids) are the same. The equilibrium contact angles, measured through fluid b, has been determined geometrically, following [dos Santos et al., 2005], by the simulation of a liquid drop in contact with a plane surface. In all the cases, fluid b is the wetting fluid and the equilibrium contact angle appears to be insensitive to the value of A. The employed parameters, written in lattice units, are summarized in Tab. 1.

In a set of computations at different saturations, all the others parameters identical, the average velocity is not an explicit parameter that could be imposed directly. Then the capillary number for that set, defined as

$$Ca = \frac{\mu \bar{\mathrm{u}}}{\sigma}, \tag{9}$$

where σ is the interfacial tension, was computed using the average velocity $\bar{\mathrm{u}}$ of a single-phase simulation with the same body force. The results for the single-phase simulation are also used to normalize the total mass flux of each species. This normalized flux is a concept equivalent to the conventional relative permeability on the assumptions that the linear relation between force and mass flux is valid for all the simulations and that the macroscopic effect of body force and pressure gradient are the same.

4. Results and discussion

A set of simulations at two different capillary numbers (Ca^I and Ca^{II}) were used to test its effect. Figure 1 shows a sequence of steady state configurations at four saturations in a completely b-wet system (θ^I).

At capillary number Ca^I and lower saturation, the fluid r first coalesces in drops that travel through the channels and then, due to periodic boundary conditions, form ganglia immobile inside the chambers. The fluid b flows through the channels and the constrictions between fluid r and walls. At $S_r = 0.4$ and $S_r = 0.6$, the fluid r is squeezed into the channels blocking the flow of both phases. In a realistic porous media the wetting phase is able to flow as a thick film even at low saturation but, due to the lack of connectivity of this solid matrix, it is trapped in channels by the non wetting fluid. With the increase of the non wetting saturation ($S_r = 0.8$), fluid r establishes some connected paths while fluid b remains immobile. The capillary equilibrium at this final configuration guarantees stable interfaces, as it is assumed in the conventional theory of two-phase flow.

At high capillary number (Ca^{II}), the configurations in steady state are completely different. For $S_r = 0.2$, the fluid r travels as drops, that eventually coalesce in the chambers and later are broken to pass through the channels. At intermediate saturations the non wetting phase forms large ganglia oriented perpendicularly to the flow direction. These large ganglia join, inducing the two phases to travel as long blobs. At $S_r = 0.8$ the interfaces are stable again, the non wetting fluid flows through connected channels and the wetting fluid remains immobile.

Figure 2 shows the normalized fluxes for capillary numbers Ca^I and Ca^{II} and the results of a third capillary number Ca^{III}, that was used to show the effect of the interface tension in the simulation. Capillary number Ca^{III} was obtained using a greater interfacial tension and fitting the value of the body force. The results are essentially equal to those of Ca^{II}, considering that the standard deviation of the normalized fluxes are inferior to 20% for all saturations. For high capillary numbers, the normalized fluxes of both phases are almost linear functions of saturation.

Figure 3 shows the steady state configuration for the θ^{II} contact angle. In this intermediate b-wet system, the final configurations are very similar to those of a system completely wet by fluid b. At low capillary number both phases are

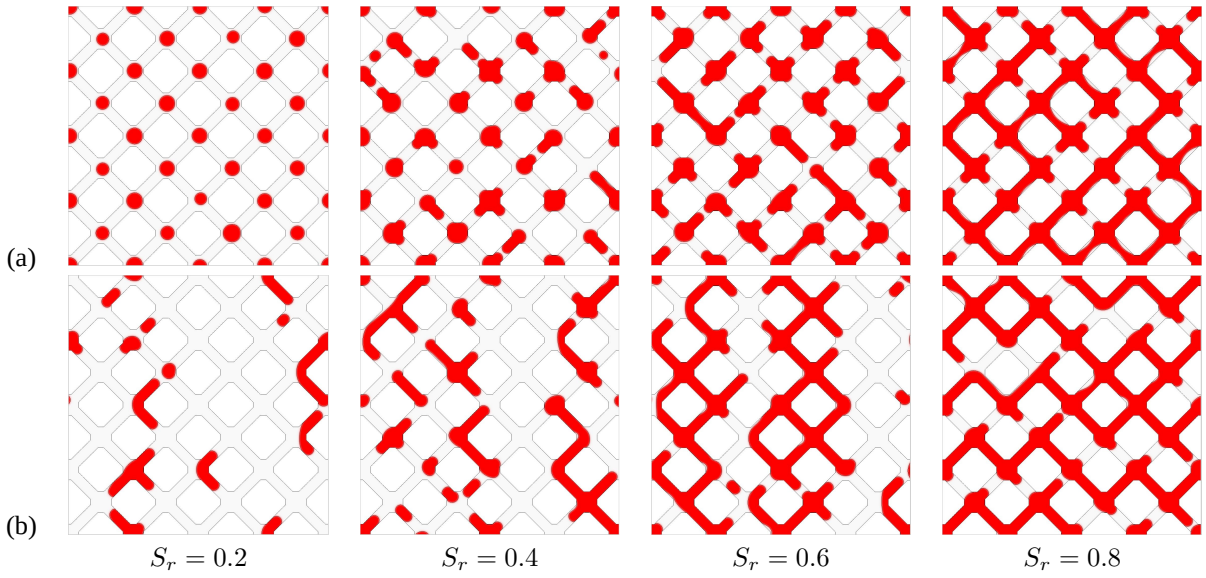

Figure 1. Steady state configurations at different saturations for a completely b-wet system. (a) Ca^I and (b) Ca^{II}. The solid is transparent, fluid b is light gray and fluid r is dark.

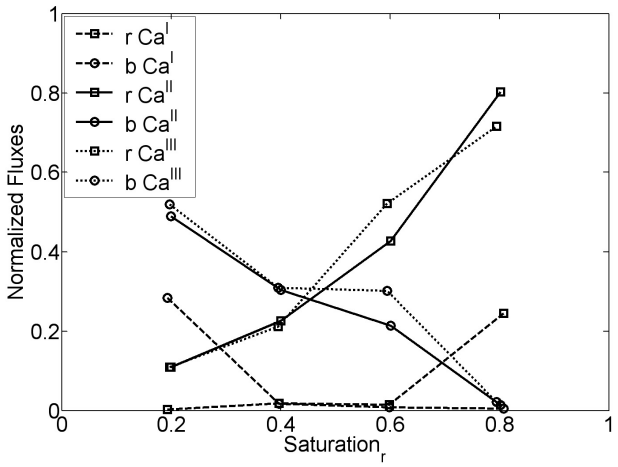

Figure 2. Normalized fluxes vs. saturation of non wetting fluid for a completely b-wet system.

mobile only through connected paths and at high capillary number the same blobs in spanwise direction are present at intermediate saturations. In the case of Ca^{II}, the normalized fluxes of both phases have a more defined linear dependence on saturation (Figure 4).

Wettability influences the relative permeabilities, controling the spatial distribution of phases in the porous media. In the simulation at low capillary number, the non wetting phase is trapped inside the chambers and, with increasing saturation of fluid r, this phase blocks the throats, lowering the flux of wetting fluid. The main difference between strong b-wet system and intermediate b-wet system appears at low saturation of the r fluid. In the case of intermediate wettability, the drops of the non wetting phase are trapped inside the chambers and also inside the throats, resulting in some paths free of obstructions and increasing the flux of the wetting phase. At high saturation of fluid r, the wetting phase is imobile, the channels formed by the non wetting fluid and the normalized fluxes are very similar for both wettabilities. The normalized fluxes curves for two wettabilities are shown in Fig. 5.

At capillary number Ca^{II}, the two phases are mobile at low r saturation. The non wetting phase enters the throats more easily in the intermediate b-wet system, blocking more passages of the wetting fluid and lowering its flux. This difference between the two systems remains until all wetting fluid are immobile. At $S_r = 0.8$, the difference in wettability has no perceptible effect in the normalized fluxes as showns Fig. 6. In a manner very similar to the experiments, the normalized flux (relative permeability) of phase b is more sensitive to wettability and decrease as the wettability of the fluid r increases [Dullien, 1992].

The identical properties of fluids r and b allow us to conclude that the system is symmetrical with relation to the

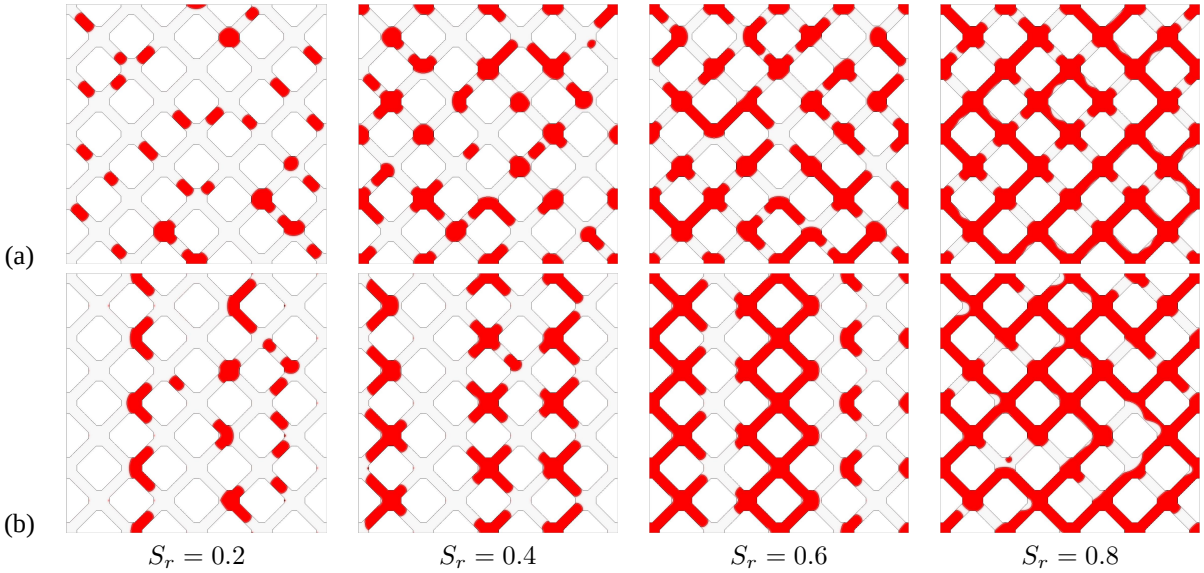

Figure 3. Steady state configurations for a intermediate b-wet system. (a) Ca^I and (b) Ca^{II}.

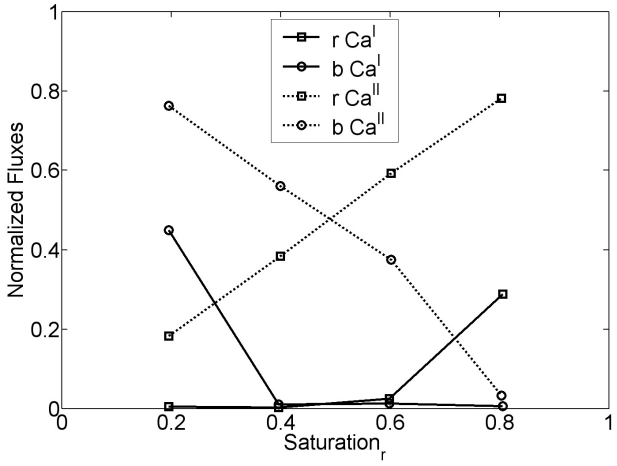

Figure 4. Normalized fluxes vs. saturation of non wetting fluid for a intermediate b-wet system.

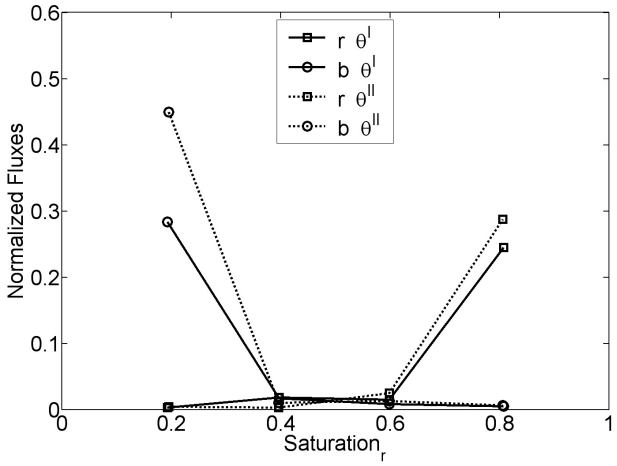

Figure 5. Normalized fluxes vs. saturation of non wetting fluid for Ca^I.

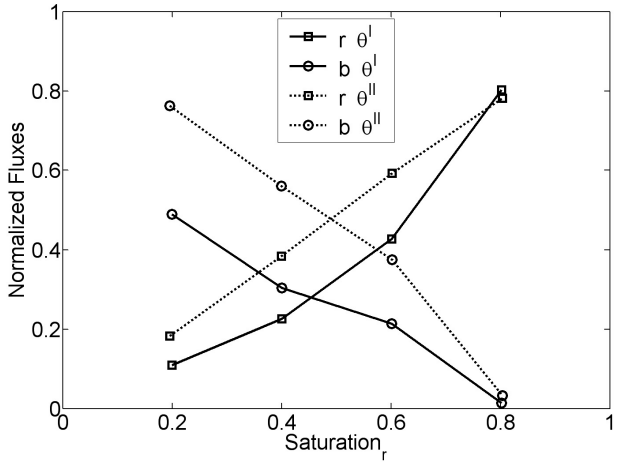

Figure 6. Normalized fluxes vs. saturation of non wetting fluid for Ca^{II}.

wettability, and that, in system of strong wettbility, the normalized flux of the non wetting phase is higher than that of the wetting phase for a given saturation.

5. Conclusions

A Lattice Boltzmann model with a split collision operator for two-phase fluid flow was implemented to study the effect of the capillary number and the wettability in the steady state relative permeability of a simplified porous medium. Roughly, the results agree qualitatively with laboratory measurements despite the artificial initial and boundary conditions and the small size of the sample. The normalized fluxes (and the relative permeabilities) increase with capillary number for all saturation and contact angles simulated.

The wetting phase appears to be more sensitive to the wettability properties of the porous media. As expected, the normalized fluxes of the wetting fluid increase at intermediate wettability for the three capillary numbers simulated. At constant capillary number, the influence of the equilibrium contact angle in relative permeability seems to be more pronounced at intermediate saturations. At low and high saturation of the non wetting fluid, this fluid forms very similar configurations for the three wettabilities studied and its relative permeability seems to be independent of the equilibrium contact angle.

As a consequence of symmetry and periodicity in spanwise direction, when capillary number is high, both phases travel as large ganglia at intermediate saturations, in a regime not observed in the experiments. Also, because of the lack of connectivity of the solid matrix the wetting fluid is trapped at high non wetting fluid saturation particularly at low capillary numbers. These discrepancies between simulations and reported experimental data are not due to the intrinsic limitations of the Lattice Boltzmann Method but to the special and simplified cases chosen for computational convenience. The LBM can handle complex pore geometries and could be used to explore the pore scale aspects of two phase fluid flow in more realistic representations of reservoir rocks.

6. Acknowledgements

The authors acknowledge the financial support of ANP (Agência Nacional do Petróleo), CNPq (Conselho Nacional de Desenvolvimento Científico e Tecnológico) and FINEP (Financiadora de Estudos e Projetos).

7. References

Avraam, D. G. and Payatakes, A. C. (1995). Flow regimes and relative permeabilities during steady-state two-phase flow in porous media. *Journal of Fluid Mechanics*, 293:207–236.

dos Santos, L. O. E., Wolf, F. G., and Philippi, P. C. (2005). Dynamics of interface displacement in capillary flow. *Journal of Statistical Physics*, In press.

Dullien, F. A. L. (1992). *Porous Media. Fluid Transport and Pore Structure*. Academic Press.

Facin, P. C. (2003). *Modelo de Boltzmann baseado em mediadores de campo para fluidos imiscíveis*. PhD thesis, Universidade Federal de Santa Catarina.

He, X. and Doolen, G. (2002). Thermodynamic foundations of kinetic theory and Lattice Boltzmann models for multiphase flows. *Journal of Statistical Physics*, 107(1/2):309.

He, X. and Luo, L. S. (1997). Theory of lattice Boltzmann method: From the Boltzmann equation to the lattice Boltzmann equation. *Physical Review E*, 56(6):6811–6817.

Olson, J. F. and Rothman, D. H. (1997). Two-fluid flow in sedimentary rock: simulation, transport and complexity. *Journal of Fluid Mechanics*, 341:343–370.

Qian, Y. H., d'Humières, D., and Lallemand, P. (1992). Lattice BGK models for Navier-Stokes equations. *Europhysics Letters*, 17(6):479–484.

Santos, L. O. E., Facin, P. C., and Philippi, P. C. (2003). Lattice-Boltzmann model based on field mediators for immiscible fluids. *Physical Review E*, 68:056302.

van Genabeek, O. and Rothman, D. H. (1996). Macroscopic manifestation of microscopic flows through porous media: Phenomenology from simulation. *Annual Review of Earth and Planetary Science*, 24:63–87.

8. Responsibility notice

The authors are the only responsible for the printed material included in this paper